Article

Thermal Analysis of Solid/Liquid Phase Change in a Cavity with One Wall at Periodic Temperature

Shogo Tomita [1], Hasan Celik [2] and Moghtada Mobedi [1,*]

[1] Mechanical Engineering Department, Graduate School of Integrated Science and Technology, Shizuoka University, Hamamatsu 432-8561, Japan; tomita.shogo.16@shizuoka.ac.jp
[2] Mechanical Engineering Department, Izmir University of Economics, 35330 Izmir, Turkey; hasan.celik@izmirekonomi.edu.tr
* Correspondence: moghtada.mobedi@shizuoka.ac.jp

Abstract: In this study, heat transfer in a square cavity filled with a Phase Change Material (PCM) under a sinusoidal wall temperature during solidification and melting is analyzed. All surfaces of the cavity are insulated except one surface, which is under the sinusoidal temperature change. The governing equations and boundary conditions are made dimensionless to reduce the number of governing parameters into two as dimensionless frequency and Stefan number. The governing equations were solved numerically by using Finite Volume Method for a wide range of Stefan number ($0.1 < Ste < 1.0$) and dimensionless frequency ($0.23 < \omega^* < 2.04$). Based on the obtained results, a chart in terms of Stefan number and dimensionless frequency is obtained to divide the heat transfer process in the cavity into three regions as uncompleted, completed, and overheated phase-change processes. For the uncompleted process, some parts of the cavity are inactive, and no phase change occurs in those parts of the cavity during the melting and freezing process. For the overheated phase change, the temperature of the cavity highly increases (or decreases), causing the sensible heat storage to compete with latent thermal storage. In the completed process, almost all thermal storage is done by the utilization of latent heat. The suggested graph helps thermal designers to avoid wrong designs and predict the type of thermal storage (sensible or latent) in the cavity without doing any computations.

Keywords: Heat transfer; solid/liquid phase change; latent thermal storage; cavity

1. Introduction

The demand for energy increases day by day as the world population increases, sharply causing a drastic increase in the emissions of greenhouse and air pollutant gases and liquids. The use of sustainable and renewable energy sources as well as the utilization of waste heat for cooling and heating purposes has attracted the attention of researchers for many years. However, there is a serious problem with using these kinds of energy sources, and that is their time-dependent character. For instance, most of the renewable energy sources are intermittent thermal sources (such as solar energy or outdoor air as an energy source). To have a continuous operated system, thermal energy in a peak period should be stored and released in demanding time. Therefore, many studies on thermal energy storage have been done and reported in the literature (e.g., [1,2]). In general, thermal energy storage systems can be classified into three groups as sensible heat storage (e.g., [3,4]), latent heat storage (e.g., [5–8]), and chemical heat storage (e.g., [9–11]). Among these groups, solid/liquids thermal energy storage has taken the attentions of researchers recently due to its simple working principle.

Thermal energy storage in cavities has been widely studied in the literature due to its wide applications in practical engineering problems. Most of the studies on phase change in a cavity have been done on steady heating or cooling wall in which wall temperature does not change over time. However, in many applications such as the use of

PCM for thermal storage of solar energy or the use of a PCM layer as thermal insulation in a wall, a periodic temperature or heat flux change exists. The number of studies on the cavities filled with PCM under a periodic temperature or heat flux is limited compared to steady temperature or heat flux imposed to a wall of the cavity. Kant et al. [12] studied the melting behavior of phase change materials (PCMs) during a cyclic heating and cooling process, computationally. A sine function of heat flux was considered at one wall of the container to provide heating and cooling of the PCMs, and the other walls of the cavity are insulated. The heat is imposed on an aluminum wall and then transferred to the fluid in the cavity. The sine function that they used for the heated/cooled surface is,

$$q_w = 250 \times \pi \times \sin\left(\pi \times \frac{t}{45}\right), \tag{1}$$

where t is time in minute and changes between 0 and 90. It was shown that despite the same amount of energy delivered to PCM, variable heating and cooling provides faster melting and solidification, respectively. Bouzennada et al. [13] did a study on a two-dimensional simulation of the melting/solidification process of a phase change material (PCM) in a square cavity. The size is 5×5 cm^2 and all cavity's walls are thermally insulated, except for the left wall on which a sine function heat flux was imposed,

$$q_w = 500 \times \pi \times \sin\left(\pi \times \frac{t}{8000}\right), \tag{2}$$

where t is time in second. It was found that the PCM melting time was shorter than the solidification time. Chabot and Gosselin [14] studied the solid-liquid phase change around a tube located in an infinite PCM domain for latent energy storage with cyclic thermal loading and unloading. Transient cyclic heat flux at the surface of the tube was imposed as,

$$q(t) = \Delta q \times \sin\left(2\pi \times \frac{t}{\tau}\right), \tag{3}$$

where q and τ are heat flux per unit length of the tube and period, respectively. Their results showed that the size of the affected region by the heating and cooling increases when the period or Stefan number increases, but it is less sensitive to the Rayleigh number. The effect of charging and discharging of multi-layers PCMs in coaxial cylinders with a time-periodic boundary condition was numerically investigated by Sadeghi et al. [15]. They assumed that the inner cylinder is subjected to a hot working fluid in which bulk temperature is changed over time. They supposed that the inner flow is a discharged heat flow from a factory with a changeable temperature over time as,

$$T_\infty = 353 + \Delta\theta \sin\left(\frac{2\pi t}{t_\tau}\right), \tag{4}$$

where $\Delta\theta$ and t_τ express the amplitude and periodicity of bulk temperature oscillation in the sinusoidal function. They declared that comparing the results for one, three, and five-layer heat exchangers shows that using the multi-layers' system due to high capacity in storing latent energy is appropriate. Rakotondrandisa et al. [16] studied melting-freezing in a cavity in which one vertical wall is at cold temperature and the temperature of the front wall changes between hot and cold temperatures for the melting and freezing processes. They declared that if the PCM does not solidify entirely, the effectiveness of the system may be considerably reduced.

Although natural convection plays an important role in solid/liquid phase change in a cavity, there are many applications in which the effect of buoyancy can be neglected. Recently the application of solid/liquid thermal storage for shuttles in space has become popular and NASA designed and produced PCM heat exchangers [17] for spacecraft thermal control. Furthermore, PCM can also be used for temperature control of electronic equipment in satellites e.g., [18]. PCM is starting to be used in micro-devices such as mobile phones and electronic equipment e.g., [19]. For small devices, the value of Rayleigh

number of the cavity in which PCM exists is small and the effect of buoyancy can be neglected.

The aim of the present study is different than the above studies. The aim of this study is to (a) minimize the number of governing parameters for a solid/liquid phase change in a cavity by using appropriate dimensionless parameters, (b) to establish a chart in terms of dimensionless parameters to predict the situation of phase change in the cavity, and (c) to recommend the best values of governing parameters in order to have high thermal storage capacity. The governing equations are expressed in dimensionless form and this leads to yielding of two dimensionless parameters as dimensionless frequency and Stefan number. Wide ranges of values for these dimensionless parameters are considered and heat transfer in the cavity is analyzed through this study. Based on the obtained results, the aimed graph in terms of Stefan number and dimensionless frequency is established. Furthermore, the ratio of the latent heat to total thermal storage in terms of two dimensionless parameters is also calculated to predict the percentage of latent thermal storage in a cavity under a period temperature change. To the best of knowledge, this study is original and presents significant hints for thermal designers of the solid/liquid phase change thermal storage systems under a periodical temperature change.

2. Problem Definition

The domain considered in this study is shown in Figure 1. The studied domain is a square cavity filled completely with PCM and the model is two-dimensional. All surfaces of the cavity are insulated except the left wall. The left wall is under a periodical temperature change. The periodic temperature of the left wall (i.e., $T_w(t)$) is expressed by the following sinusoidal function.

$$T_w = f(t) = T_0 + a \sin(\omega t), \tag{5}$$

where T_0 is the initial temperature of the PCM, a is the amplitude, and ω is frequency of the applied sinusoidal temperature change.
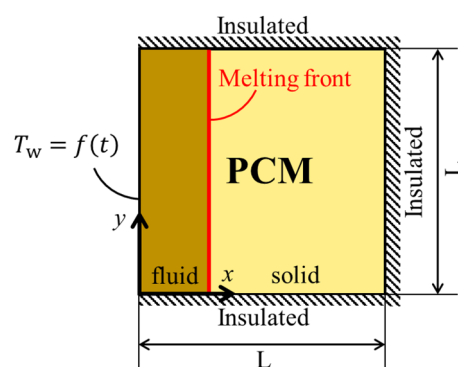

Figure 1. The studied cavity and boundary conditions.

The employed PCM is Paraffin (RT35HC) and the thermophysical properties of the PCM are presented in Table 1. Assumptions that are used in this study are a) all thermophysical properties for the PCM are constant and do not change with temperature, b) gravity does not play an important role in the heat transfer (the Rayleigh number is small), c)the radiation heat transfer is neglected.

.

Table 1. The thermal properties of the Paraffin RT35HC considered in this study [20].

Solid and liquid phase density (kg/m^3)	825
Thermal conductivity (W/mK)	0.2
Specific heat capacity (J/kgK)	2000
Latent heat (J/kg)	240000
Melting range as T_{ms}-T_{mf} (K)	307.15–309.15
Dynamic viscosity (kg/ms)	0.00258

Figure 2 shows the process of heat transfer during the thermal storage through the cavity, schematically. It illustrates the change of temperature in the cavity near hot wall with time. If the temperature of PCM is less than T_{ms}, the region is solid. The phase of PCM is liquid when the temperature of PCM is greater than T_{mf}. The PCM is under melting in the region between T_{ms} and T_{mf}. The amplitude and period are also shown in Figure 2. As it can be seen, there are two processes in solid/liquid thermal storage systems, as charging and discharging processes. Each process consists of two types of heat storage as sensible and latent heat storage. Hence, the total thermal storage is the summation of sensible and latent heat storage for each process.
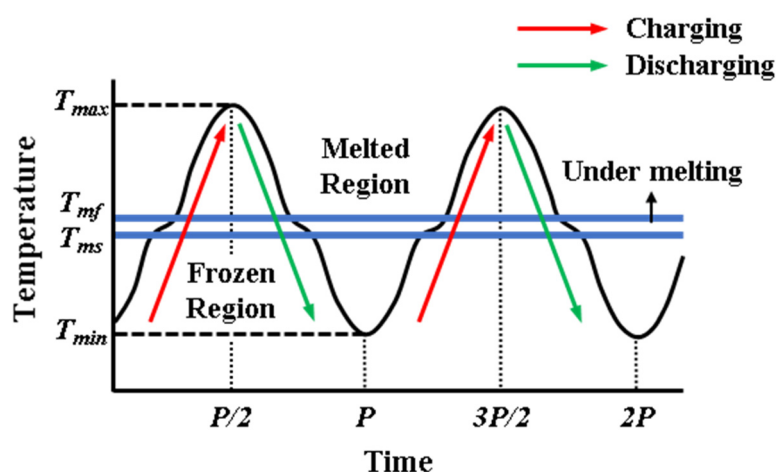
Figure 2. Schematic view of temperature change with time in the cavity near hot wall.

The present study was performed for wide range of Stefan number (0.1 < Ste < 1.0) and dimensionless frequency (0.23 < ω^* < 2.04). Table 2 is presented to show the corresponding minimum and maximum dimensional values of Stefan and dimensionless frequency in the present study. The initial temperature (T_0) and length of the square cavity were 308.15 K and 0.01 m, respectively, for all runs of this study.

Table 2. The values of dimensional parameters and corresponding dimensionless numbers used in this study.

$T_{max} - T_{min}$	Period (s)	Ste	ω^*
12	25374	0.1	0.23
12	2537.4	0.1	2.04
120	25,374	1.0	0.23
120	2537.4	1.0	2.04

3. Governing Equations and Boundary Conditions

The dimensional and dimensionless governing equations are described separately in this section.

3.1. Dimensional Governing Equation

Since the motion of fluid in the cavity is not considered, the dimensional form of the energy equation for the problem can be written as:

$$\frac{\partial T}{\partial t} = \frac{k}{\rho c_p}\left(\frac{\partial^2 T}{\partial x^2} + \frac{\partial^2 T}{\partial y^2}\right) + \frac{1}{c_p}\Delta H \frac{\partial \sigma}{\partial t},$$ (6)

where ΔH and σ refer to the latent heat of PCM and melting fraction in the slurry region, respectively. The melting starts at temperature of T_{ms} and finishes at T_{mf} temperature. The region below T_{ms} is the frozen phase of PCM while the region above T_{mf} refers to the melted region. The region between T_{ms} and T_{mf} is the region where melting occurs. The value of σ is "0" for the frozen region and "1" for the melted region. The derivatives of σ when the temperature is not between T_{ms} and T_{mf} with respect to time are zero, which means that there is no source term for the completely frozen and melted regions while it changes between 0 and 1 in the melting/freezing region.

The cavity is fully filled with PCM and all surfaces of the cavity are insulated except one surface, which is under a periodical temperature change. Considering Figure 1, the initial and boundary conditions can be expressed mathematically as follows:

$$x = 0 \quad T = T_0 + a\sin(\omega t)$$
$$x = L \quad \frac{\partial T}{\partial x} = 0$$
$$y = 0, L \quad \frac{\partial T}{\partial y} = 0$$
$$t = 0 \quad T = T_0,$$ (7)

where T_0, a, and ω are initial temperature, amplitude, and frequency of the heated wall. As it is well known, the period can be defined as $\tau = 1/\omega$, where p is period with unit of second in this study.

3.2. Dimensionless Governing Equation and Boundary Conditions

The dimensionless form of the energy equation written in the previous section, in Equation (6), can be written as follows

$$\frac{\partial \theta}{\partial Fo} = \frac{\partial^2 \theta}{\partial x^{*2}} + \frac{\partial^2 \theta}{\partial y^{*2}} + \frac{1}{Ste}\frac{\partial \sigma}{\partial Fo}.$$ (8)

The following dimensionless parameters are used in order to make Equation (6) dimensionless,

$$x^* = \frac{x}{L}, \quad y^* = \frac{y}{L}, \qquad Fo = \frac{\alpha t}{L^2}, \qquad \theta = \frac{T - T_o}{T_{max} - T_{min}}, \qquad Ste = \frac{C_p \Delta T}{\Delta H},$$ (9)

where the dimensionless temperature and time are shown by θ and Fo, respectively. Ste represents Stefan number referring to the ratio of the latent heat to sensible heat stored by PCM. T_{max} and T_{min} are the highest and lowest of the temperature of the wall during the sinusoidal variation of temperature as shown in Figure 2. The dimensionless form of the initial and boundary conditions is given as,

$$x^* = 0 \qquad \theta = \theta_w = \frac{1}{2}\sin(\omega^* Fo)$$
$$x^* = 1 \qquad \frac{\partial \theta}{\partial x^*} = 0$$
$$y^* = 0, 1 \qquad \frac{\partial \theta}{\partial y^*} = 0$$
$$Fo = 0 \qquad \theta = 0.$$ (10)

In the above equation, ω^* is the dimensionless frequency and it is defined as:

$$\omega^* = \frac{\omega L^2}{\alpha}.$$ (11)

From Equations (9) and (10), it can be concluded that there are two dimensionless governing parameters, as Stefan number and dimensionless frequency affect the results of this problem. The use of dimensionless parameters (Equation (9)) reduces the number of dimensional variables (α, L, a, w, ΔH, T_0) to two parameters as ω^* and Ste. It should be mentioned that the dimensionless period is shown by τ in this study and it is clear that $\omega^* = 1/\tau$. The value of Stefan number changes between 0.1 and 1.0 while the dimensionless frequency ω^* varies between 0.23 and 2.04.

4. Computational Details

The heat conduction equation is solved numerically by using OpenFoam 6 software using Finite Volume Method. The number of square mesh was 100×100. Our computational study showed that it is sufficient to divide a period to 100,000-time steps to obtain accurate results. Therefore, the time interval was not constant in this study and changed by the value of the period. "chtMultiRegionFoam" which is a solver of OpenFoam, was used to solve the governing equation. This solver can be used for unsteady single-phase flow as well as for unsteady conjugate heat and fluid flow. In order to solve the source term of Equation (6), a sub-program of OpenFoam named as "solidificationMelting-Source" was added to chtMultiRegionFoam solver. The relaxation factor was fixed as 0.5 for all runs of this study. The absolute and relative tolerances were 10^{-9} and 0.0001, respectively. Parallel processing (with 6 cores) was used to reduce the run time. The value of "nOuterCorrectors" showing the number of iterations at each time step was 30. No convergence criterion is needed to stop the program since the problem is a time-dependent periodic problem. The program was terminated when enough cycles were done to obtain steady periodic results. The program was stopped time by time to check whether the steady periodic results were achieved. The checking was done by plotting and observing the temperature at three points of $x^* = 0.01$, 0.5, and 0.98 through all cycles. The running of the program continued until it reached a steady periodic result.

Grid independency for the employed time interval was checked. Figure 3a shows the performed study for mesh independency. Since the convection heat transfer is neglected, it is possible to obtain accurate results with a small number of mesh. As it can be seen from Figure 3a, the results of 20×20 mesh overlap the obtained values of 100×100 mesh number. In this study, 100×100 mesh is used to prevent the possibility of any wrong results due to the number of mesh. Figure 3b shows the study done to check the time interval. The results of $\tau/10{,}000$ and $\tau/100{,}000$ match each other. In this study $\tau/100{,}000$ is used to be sure of the accuracy of the obtained results.

One of the difficulties in the performed computations is the long run time. An initial condition is assigned to the software, however, to obtain steady periodical changes for the temperature, a long running time is required. Figure 3 shows the change of temperature variation at $x = L$ (or $x^* = 1$) during a run for the problem with $\omega^* = 2.04$ and Ste = 0.6. As it can be seen, at least 17 melting and freezing cycles should be finished in order to have a steady periodical cycle. In this study, it is accepted that a steady periodical change in the cavity exists when the variation of temperature at $x^* = 0.01$, 0.5 and 0.98 becomes periodically steady (see Figure 4) .
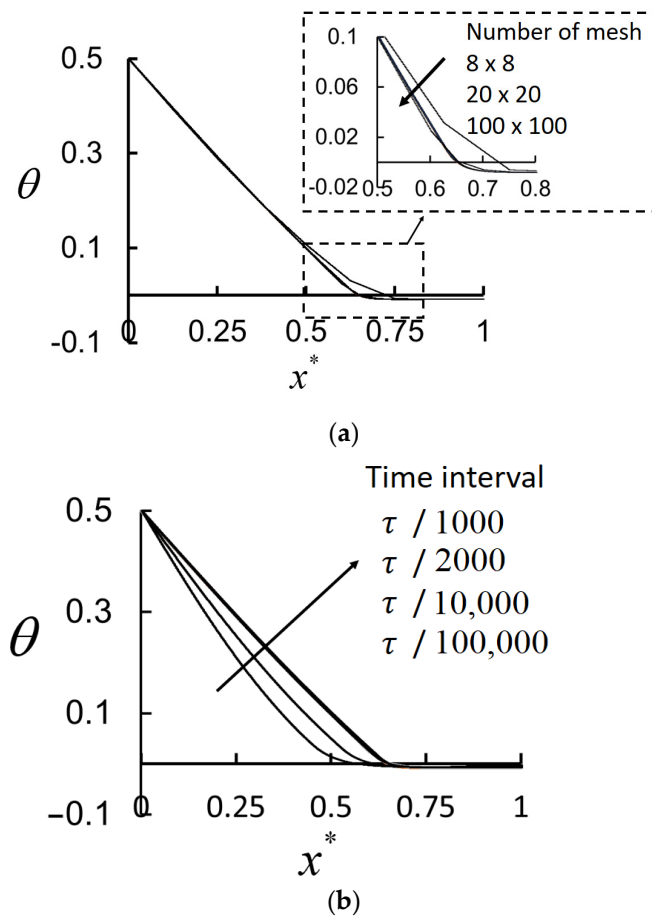
Figure 3. Mesh and interval time independency study for Ste = 0.6 and $\omega^* = 2.04$ by using temperature at the line of $Y^* = 0.5$ when the wall temperature is maximum (T_{max}), (**a**) mesh independency (**b**) time interval independency.
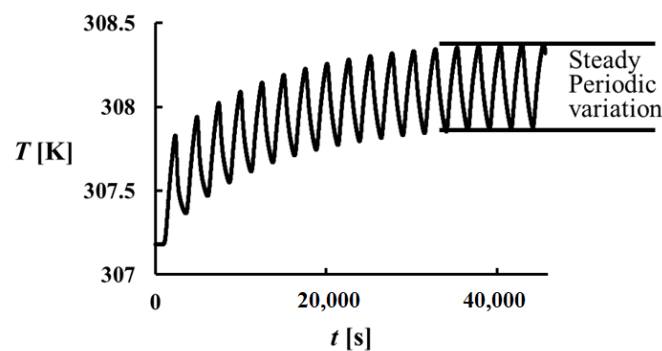
Figure 4. The change of temperature at x = 0.98 from initial state to the ending of a run (17 cycles).

The total melting time (Fo_{total}) is calculated when the PCM in the entire cavity melts, in other words when $\sigma = 1$ for the entire cavity. Heat storage in the cavity consists of sensible and latent heat storage. That is why a parameter as the ratio of latent heat storage is defined and used in this study,

$$\eta = \frac{Q_{latent}}{Q_{total}},$$ (12)

where Q_{latent} and Q_{total} are latent and total heat storage in the cavity for a period, and η shows the ratio of latent heat storage. The minimum value of η is zero, indicating that

all stored heat is done by sensible storage while it is 1 (i.e., $\eta = 1$) showing that all stored heat is performed by latent heat storage. The value of Q is calculated by the following equation

$$Q_{total} = q".A = A.\int_0^\tau -k_{pcm}\frac{dT}{dx}dy.$$

(13)

A is the heat transfer area of the heated/cooled cavity, which is A = L. 1 (m^2). The latent heat is found by subtraction of latent heat and sensible heat transfer rates.

$$Q_{latent} = Q_{total} - Q_{sensible}.$$

(14)

Sensible heat can be easily calculated from the following equation,

$$Q_{sensible} = mC_p(T_{av,max} - T_{av,min}),$$

(15))

where m is the mass of PCM inside the cavity. $T_{av,max}$ and $T_{av,min}$ are the maximum and minimum average temperature in the cavity during the last cycle.

5. Validation Study

For the validation study, the melting of a PCM under pure heat conduction in a semi-infinite medium is analyzed as shown in Figure 5. Initially, the domain is at T_{in} and suddenly the temperature of the left wall becomes T_h where $T_{in} < T_h$. The melting temperature of PCM (i.e., T_m) is between T_h and T_{in}. The energy equation for this problem is 1D heat conduction with solid/liquid phase change. There are two temperatures for this problem as the temperature of the frozen phase (T_s) and the temperature of the melted phase (T_f). The analytical solution of energy equation for this problem is presented in literature and equations for T_s and T_f were found as [21],

$$T_s(x,t) = T_{in} + (T_m - T_{in})\frac{erfc\left(\frac{x}{2\sqrt{\alpha_s t}}\right)}{erfc(\gamma\lambda)}, x \geq X, t > 0,$$

(16)

$$T_f(x,t) = T_h + (T_h - T_m)\frac{erf\left(\frac{x}{2\sqrt{\alpha_f t}}\right)}{erf(\lambda)}, 0 \geq x, t > 0,$$

(17)

where x is the location for which the temperature is required. γ is thermal conductivity ratio as $\gamma = \sqrt{\alpha_s / \alpha_f}$ and $X(t)$ shows the position of the interface between the solid and fluid, and it is defined by the following equation,
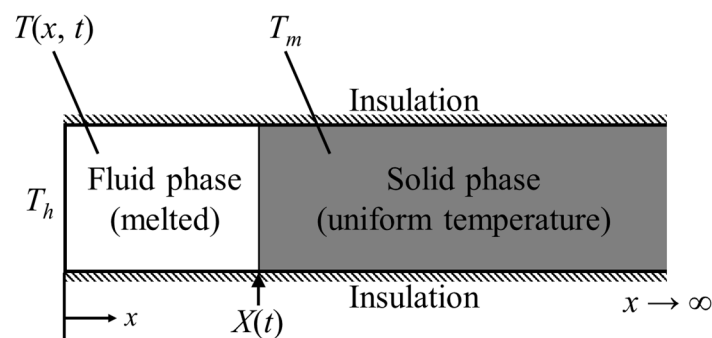
$$X(t) = 2\lambda\sqrt{\alpha_f t}.$$

(18)

The coefficient of λ is the root of the following equality,

$$\frac{Ste_f}{\exp(\lambda^2)\,erf(\lambda)} - \frac{Ste_s}{\gamma\exp(\gamma^2\lambda^2)erfc(\gamma\lambda)} = \lambda\sqrt{\pi}.$$

(19)

Ste_f and Ste_s are Stefan number for the melted and unmelted regions and defined as,

$$Ste_f = \frac{Cp_f(T_h - T_m)}{\Delta H}, Ste_s = \frac{Cp_s(T_m - T_{in})}{\Delta H}.$$

(20)

Figure 5. Melting in a semi-infinite domain with initial temperature of T_{in} .

For the same problem, the computational results were found by using OpenFoam 6 software. A rectangular domain with a length of 500 mm and height of 10 mm is considered. Since the length of the domain is too long, the domain can be accepted as a one-dimensional semi-infinite heat conduction. The numerical results of the study are valid for the region near the heated surface since it is too far from the end surface and the end effect is small in this region. The number of mesh in transverse direction is not important since the problem is one dimensional, but the number of mesh in x-direction was 1000. The time interval for obtaining an accurate solution was 1 s. The problem is solved for RT35HC PCM for which the thermophysical properties are shown in Table 1. Since we have one melting temperature in the analytical solution, the melting temperature is considered as the average of T_{ms} and T_{mf} . Figure 6 shows the comparison of the analytical and numerical solutions and as it can be seen that a good agreement between them exists indicating sufficient accuracy of the results of the present study.
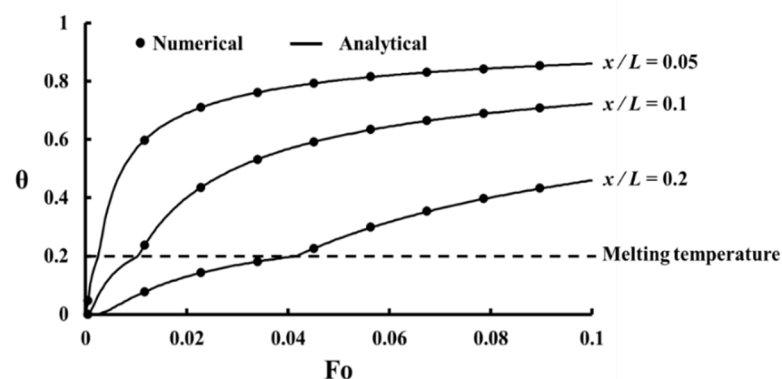
Figure 6. The comparison of the present computational study results with the obtained analytical results from Equations (16) and (17).

6. Results and Discussion

To discover how heat flow changes by time in the cavity, the change of temperature and melting fraction at three points as $x^* = 0.01, 0.5$ and 0.98. are plotted. Therefore, it is possible to discover the variation of heat flow in three regions as (a) the region close to the hot wall, (b) the middle region, and (c) the right wall region, which is far from the heat source. The plotted figures show how these regions are affected by the sinusoidal variation of temperature at the hot wall. The obtained results and plotted diagrams discussed are presented below.

The change of temperature and the melting fraction in the cavity with Ste = 0.6 and $\omega^* = 2.04$ for different instants of a period is shown in Figure 7a,b. As it can be seen there

is no melting when $Fo = 0\tau$ but by increasing time, the melting from the left wall approaches to the right wall, which is insulated ($Fo = 1/4\ \tau$ and $2/4\ \tau$). By decreasing wall temperature, freezing starts from the left wall while the right region of the cavity is hotter than left wall region. This time, freezing starts to move from the left region to the right region and reduces the temperature of the right region. It can be seen that the temperature in the region close to the right wall does not change and the maximum temperature change exists in the left region. It seems that melting in the right wall is negligible and it behaves like a dead region. Figure 7c shows the change of temperature at three points inside the cavity as $x^* = 0.01, 0.5,$ and 0.98. A large variation of temperature can be seen for the point of $x^* = 0.01$ which is close to the heated wall. The temperature at the center does not highly change but it exceeds the PCM melting range showing that complete freezing and melting process occurs in the middle region (i.e., latent heat is stored). However, for the points of $x^* = 0.98$ there is almost no change of temperature, and the phase of this region is between solid and fluid (slurry region) and almost no heat is stored by this region. Hence, the right region is almost inactive, and it does not play a significant role in the thermal storage, however it occupies space in the cavity. Figure 7d shows all details of the melting and freezing process. It shows the change of melting ratio (i.e., σ) with dimensionless time for the same three points. For the point of $x^* = 0.01$, a complete melting and freezing is seen. Even, the phase of this region does not change (it is solid or liquid) for a long time and this region becomes overheated (for melting period) or subcooled (for the freezing period). For the point of $x^* = 0.5$, again a complete melting and freezing process is seen, however, there is a negligible overheating or subcooling process for the central region. Therefore, complete latent heat storage exists for this region. However, for the point of $x^* = 0.98$, the view is different. There is a small change of σ, showing that this region does not play a significant role in thermal storage and that is why the right region can be called a dead region. This region just occupies space without storing energy causing reduction of thermal storage power.

The change of temperature and melting ratio in the cavity with Ste = 0.6 and $\omega^* = 0.23$ is shown in Figure 8a,b. Similar to Figure 7a,b, the melting starts from the left wall and moves to the right wall. However, it seems that the temperature of the right region increases extremely, and it becomes highly above the melting temperature ($Fo = 1/4\ \tau$) and almost a uniform temperature exists. In other words, the right region is overheated, and it seems that the sensible heat is considerably stored. By reducing the temperature at the left wall, freezing starts from this wall and approaches to the right region. This time, the cavity becomes considerably lower than the melting point ($Fo = 3/4\ \tau$) and again a uniform low temperature exists in the entire cavity. The variations of temperature at $x^* = 0.01$, 0.5 and 0.98 points are also plotted and shown in Figure 8c. As it can be seen, not only the temperature change at $x^* = 0.01$ is considerable but also a high variation of temperature for the points $x^* = 0.5$ and 0.98 exists. Figure 8 shows that in addition to latent heat, the sensible heat storage is considerably stored in the PCM during the process. The change of σ with τ can be seen from Figure 8d. The latent heat is also stored in the entire cavity, however as it is mentioned before, it seems that sensible heat storage for this case may compete with the stored latent heat.
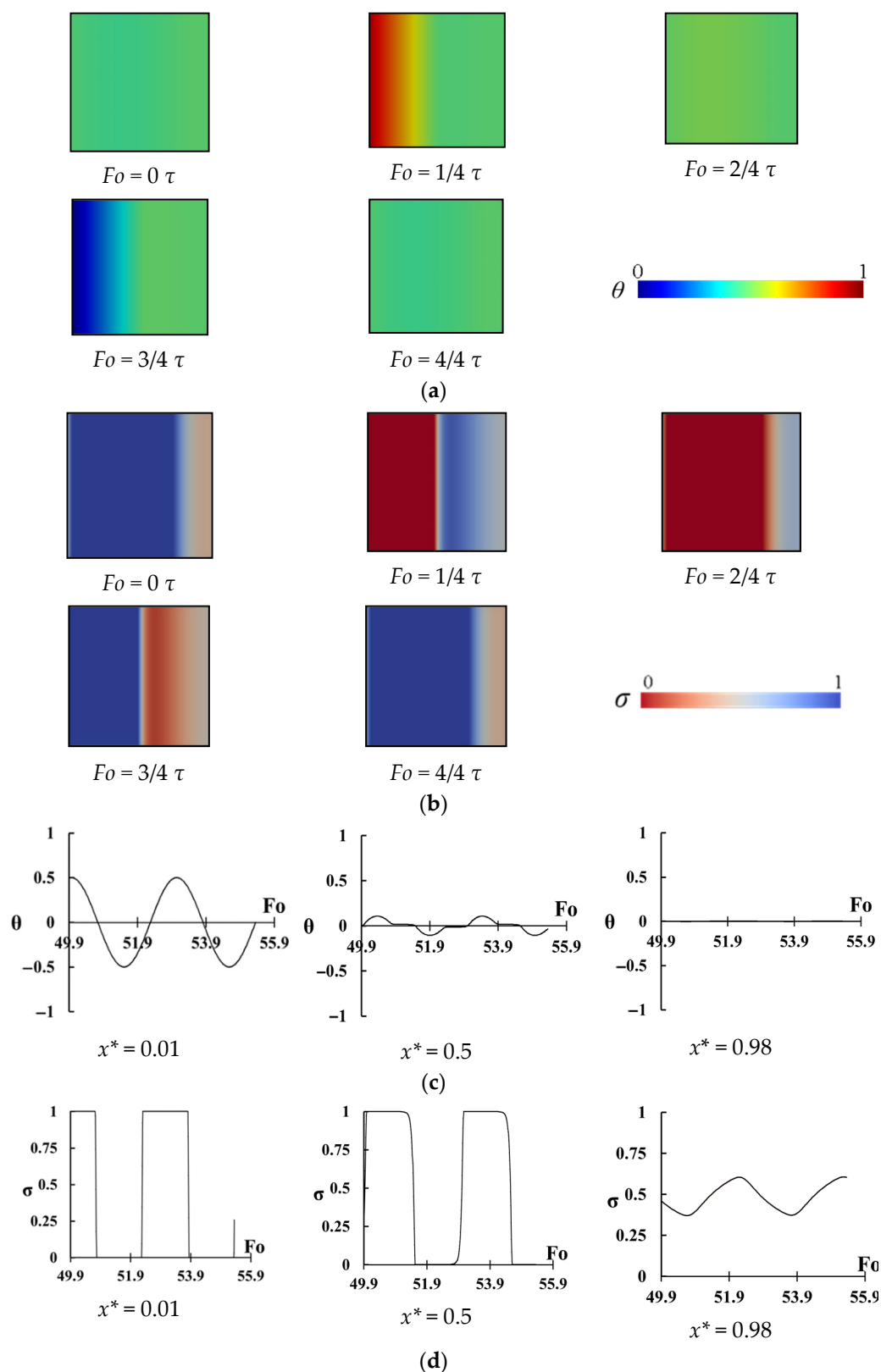
Figure 7. Melting and freezing of PCM in the cavity when Ste = 0.6 and ω^* = 2.04 at different time steps of a period, (**a**) temperature distribution, (**b**) melting fraction distribution, (**c**) temperature changes at three different points for the last two periods, (**d**) melting fraction change at three different points for the last two periods.
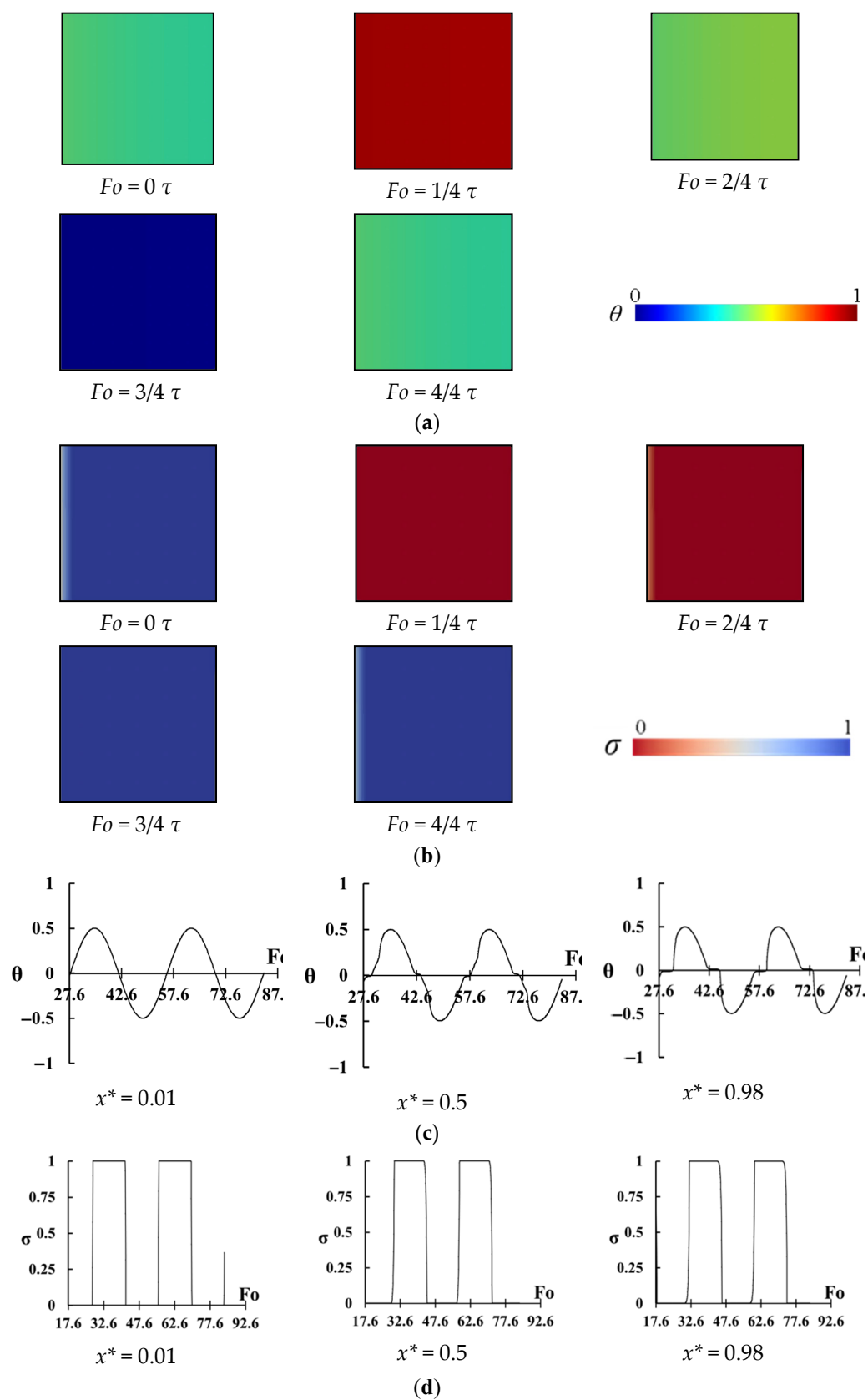
Figure 8. Melting and freezing of PCM in the cavity when Ste = 0.6 and ω^* = 0.23 at different time steps of a period, (**a**) temperature distribution, (**b**) melting fraction distribution, (**c**) temperature changes at three different points for the last two periods, (**d**) melting fraction change at three different points for the last two periods.
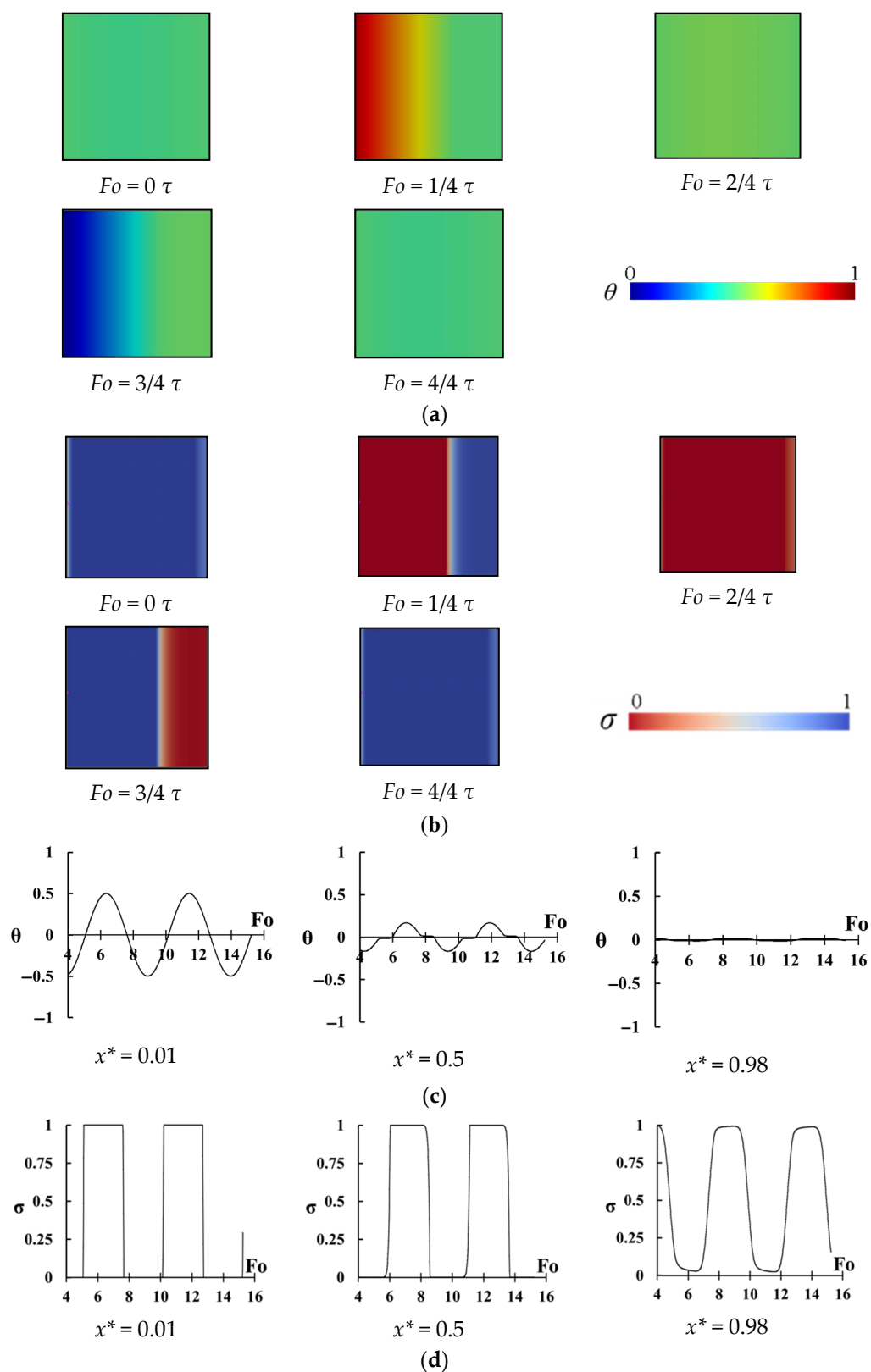
The same temperature distributions of Figures 7 and 8 are shown in Figure 9 but for $\omega^* = 1.24$. The melting and freezing start from the left wall and approach to the right region. The difference between Figures 7 and 8 with Figure 9 is that it seems that PCM is completely melted or frozen on time in the right region. In Figure 7, the melting and freezing of PCM are not completed and in Figure 8 the melted PCM in the right region remains in the same phase for a long time and stores sensible heat. However, for Figure 9, most of the heat in the right region is stored by latent heat, and almost no sensible heat is stored. The variation of temperature and melting fraction for three points of $x^* = 0.01, 0.5$ and 0.98 prove this fact (Figure 9c,d). A high-temperature change can be seen for the point of $x^* = 0.01$, and this temperature variation considerably decreases for $x^* = 0.98$, however, a complete solid/liquid phase change occurs in the right region since the temperature changes just inside the melting temperature region. Almost a full phase change can be seen in Figure 9d for $x^* = 0.98$.

As it can be seen from Figures 7–9, based on the values of ω^* and Ste number, there might be three regions as (a) the region in which the phase change in the right region (i.e., end of the cavity) does not occur completely, (b) the region in which the right region stays in the same phase for a long time and (c) the region in which the phase change occurs in the entire cavity with minimum temperature change. In this study, a chart in terms of dimensionless frequency and Ste number is established to predict the character of the phase change in the cavity without doing any computational calculation, and it is shown in Figure 10. The x-axis is dimensionless frequency while y-axis shows Ste number. The plotted line divides the chart into three regions. The top region is called the overheated/cooled process, referring to a process that the entire region of the cavity is overheated or subcooled. The bottom region is called the uncompleted process and the right region of the cavity is inactive and just occupies space and increases the weight. The operation conditions on the curve show a cycle in which the right region of the cavity is under complete solid/liquid phase change without any overheating or subcooling. Figure 10 yields three important points,

(a) A thermal designer should calculate values of ω^* and Ste number and find operation points on Figure 10. She/he should avoid operation in the uncompleted process region since some parts of the cavity are inactive and do not play any role in thermal storage;

(b) For the points which are on the line (completed process), most of the thermal storage occurs by latent heat while for the system operating in the overheated/cooled process, in addition to latent heat, sensible thermal storage also plays an important role;

(c) In many cases, Stefan number is accepted as a dimensionless number used to decide the role of latent heat in thermal storage. For instance, for the low values of Stefan number, the role of latent thermal storage is significant while high Stefan numbers of sensible thermal storage gain importance. Figure 10 shows that if a periodical temperature change exists at a wall of a thermal storage cavity, in addition to Stefan number, dimensionless frequency should be taken into account. For instance, one may think that sensible heat storage for a cavity with Ste = 1 is significant, however our results show that for Ste = 1 and $\omega^* = 2.04$, most of the heat is stored by latent heat rather than sensible thermal storage.

Figure 9. Melting and freezing of PCM in the cavity when Ste = 0.6 and ω^* = 1.24 at different time steps of a period, (**a**) temperature distribution, (**b**) melting fraction distribution, (**c**) temperature changes at three different points for the last two periods, (**d**) melting fraction change at three different points for the last two periods.
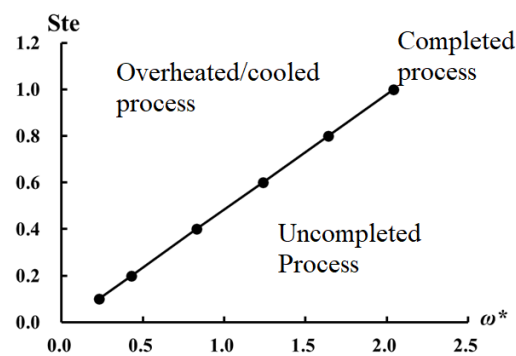
Figure 10. The position of defined three processes in terms of ω^* and Stefan number.

The change of percentage of latent heat in the stored thermal energy (i.e., as the ratio of latent heat storage) with dimensionless frequency for the region of overheated/cooled process is calculated for three Ste numbers as 0.2, 0.6, and 1.0 and shown in Figure 11. The value of η changes between 0 and 1. η = 0 refers to 100% sensible heat storage while η = 1 shows a process only with latent heat storage. The value of η for the completed process is also calculated and shown. This diagram shows that a) the possibility of latent thermal storage even for a process with a high Stefan number (for instance Ste = 1 and ω^* = 2.04) exists, but in general, the effect of latent heat on thermal storage is greater than sensible storage for the process with small Stefan number (e.g., Ste < 0.4).

Figure 11 shows that by decreasing ω^* the ratio of latent heat storage decreases. For instance, for Ste = 0.6, 95% of the stored heat is latent heat when ω^* = 1.24 but by reducing the dimensionless frequency to 0.23, the weight of latent heat in the process decreases to 60%. By decreasing of ω^*, the temperature of the cavity highly increases or decreases as is shown in Figure 8. PCM are used in a thermal storage process due to their latent heat. However, for the process with a high value of Stefan number (Ste = 1) and low dimensionless frequency (such as ω^* = 0.23), the role of latent heat is 48%. Therefore, in those processes, the use of proper sensible thermal storage materials may increase the thermal storage performance. The reason for low latent thermal storage is not Stefan number and this effect is due to the low value of dimensionless frequency (i.e., long period).
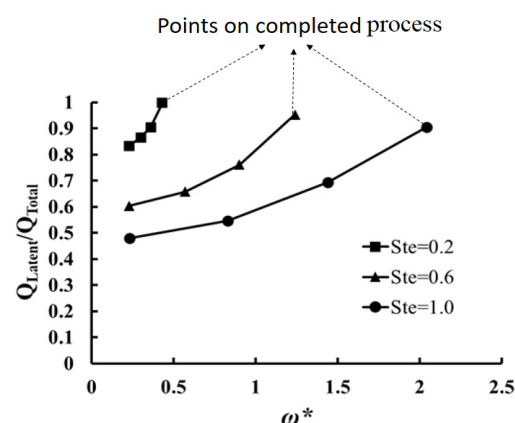

Figure 11. The change of percentage of stored latent heat with ω^* for the three Stefan numbers.

7. Conclusions

The problem of freezing and melting in a cavity under a sinusoidal wall temperature change is investigated. The effect of gravity is neglected and the heat conduction equation for the problem is solved. The suggested method for non-dimensionalization of governing equation, initial and boundary conditions reduce the number of dimensional parameters

into two dimensionless parameters providing the analysis of the problem easier. The heat conduction equation is solved for a wide range of Stefan and dimensionless frequency. The following remarks can be concluded from the obtained results,

(a) Based on the dimensionless frequency and Stefan number, three different cases can be observed. In some cases, such as (dimensionless frequency of 2.04 and Stefan number of 0.6), the right region of the cavity is inactive and does not play any role on latent heat thermal storage (uncompleted region). For some studied cases (such as dimensionless frequency of 0.23 and Stefan number of 0.6), the right region of the cavity is overheated or sub-cooled, causing the increase of sensible heat storage (overheated/subcooled region). However, for specific values of dimensionless frequency and Stefan number, a complete phase change occurs in the right region of the cavity without considerable overheating and sub-cooling (completed process).

(b) Based on the established chart, thermal designers should not design a cavity whose operating point is in the uncompleted region (such as dimensionless frequency of 2.04 and Stefan number of 0.6).

(c) For a considered Stefan number, the effect of latent heat increases by increasing dimensionless frequency.

(d) For high values of Stefan number (i.e., Stefan number of 1.0) and low dimensionless frequency (i.e., dimensionless frequency of 0.23), the effect of latent heat thermal storage may be small, hence the use of a proper sensible thermal storage material may provide better thermal storage.

The results of the present study are useful for the design of solid/liquid phase change for cavities under a periodic time dependence boundary condition for applications such as satellites or small electronic devices such as mobile phones. Further studies on the same topic by using the effect of convection in the cavity must be done to help thermal storage designers for better design when gravity affects heat transfer in the cavity.

Author Contributions: Conceptualization, M.M.; methodology, M.M.; software, S.T and H.C.; validation, S.T.; formal analysis, S.T., H.C. and M.M.; investigation, S.T., H.C. and M.M.; writing—original draft preparation, S.T, H.C. and M.M.; writing—review and editing, S.T, H.C. and M.M.; visualization, S.T, H.C.; supervision, M.M; All authors have read and agreed to the published version of the manuscript.

Nomenclature

a	Amplitude of temperature [K]
C_p	Specific heat capacity [J/kg K]
Fo	Fourier number [-]
g	Gravity [m/s^2]
ΔH	Latent heat of fusion [J/kg]
k	Thermal conductivity [W/m K]
L	Length of cavity [m]
P	Dimensional period [s]
Q	Heat storage [J]
q	Heat flux [W]
Ste	Stefan number [-]
T	Temperature [K]
t	Time [s]

$X(t)$	Location of the solid-fluid interface [m]
x, y, z	Cartesian coordinates [m]
Greek symbols	
α	Thermal diffusivity [m²/s]
γ	Square root of thermal diffusivity ratio of fluid and solid phases [-]
η	Heat storage ratio [-]
θ	Dimensionless temperature [-]
λ	Root of Equation (12)
ρ	Density [kg/m³]
σ	Melting ratio [-]
τ	Dimensionless period [-]
ω	Angular frequency of temperature [rad/s]
Subscripts and superscripts	
0	Initial
f	Fluid
m	Melting
mf	Melting finishes
ms	Melting starts
s	Solid
w	Wall
$*$	Dimensionless

References

1. Lu, Y.; Hooman, K.; Atrent, A.D.; Russell, H. An Experimental Facility to Validate Ground Source Heat Pump Optimisation Models for the Australian Climate. *Energies* **2017**, *10*, 138.
2. Manchin, S.; Noro, M. Reversible Heat Pump Coupled with Ground Ice Storage for Annual Air Conditioning: An Energy Analysis. *Energies* **2020**, *13*, 6182.
3. Cisek, P.; Taler, D. Numerical and experimental study of a solid matrix Electric Thermal Storage unit dedicated to environmentally friendly residential heating system. *Energy Build.* **2016**, *130*, 747–760.
4. Taler, D.; Dzierwa, P.; Trojan, M.; Sacharczukb, J.; Kaczmarskib, K.; Talerb, J. Mathematical modeling of heat storage unit for air heating of the building. *Renew. Energy* **2019**, *141*, 988–1004.
5. Chunyang, W.; Mobedi, M. A comprehensive pore scale and volume average study on solid/liquid phase change in a porous medium. *Int. J. Heat Mass Transf.* **2020**, *159*, 120102.
6. Bondareva, N.S.; Ghalambaz, M.; Sheremet, M.A. Influence of the Fin Shape on Heat Transport in Phase Change Material Heat Sink with Constant Heat Loads. *Energies* **2021**, *14*, 1389.
7. Chunyang, W.; Mobedi, M. A new formulation for non-dimensionlization heat transfer of phase change in porous media: An example application to closed cell porous media. *Int. J. Heat Mass Transf.* **2020**, *149*, 119069.
8. Ochman, A.; Chen, W.Q.; Błasiak, P.; Pomorski, M.; Pietrowicz, S. The Use of Capsuled Paraffin Wax in Low-Temperature Thermal Energy Storage Applications: An Experimental and Numerical Investigation. *Energies* **2021**, *14*, 538.
9. Ilis, G.G.; Demir, H.; Saha, B.B. Innovative approach in adsorption chiller: Combination of condenser-adsorber for improving performance. *Appl. Therm. Eng.* **2021**, *192*, 25.
10. Gediz, G.I.; Mobedi, M.; Ulku, S. A dimensionless analysis of heat and mass transport in an adsorber with thin fins; uniform pressure approach. *Int. Commun. Heat Mass Transf.* **2011**, *38*, 790–797.
11. Demir, H. Development of microwave assisted zeolite–water adsorption heat pump. *Int. J. Refrig.* **2013**, *36*, 2289–2296.
12. Kant, K.; Shukla, A.; Sharma, A.; Biwole, P.H. Melting and solidification behavior of phase change materials with cyclic heating and cooling. *J. Energy Storage* **2018**, *15*, 274–282.
13. Bouzennada, T.; Mechighel, F.; Filali, A.; Kolsi, L. Study of the usability of sinusoidal function heat flux based on enthalpy-porosity technique for PCM-related applications. *J. Therm. Anal. Calorim.* **2020**, *141*, 1769–1784.
14. Chabot, C.; Gosselin, L. Solid-liquid phase change around a tube with periodic heating and cooling: Scale analysis, numerical simulations and correlations. *Int. J. Therm. Sci.* **2017**, *12*, 345–357.
15. Sadeghi, H.M.; Babayan, M.; Chamkha, A. Investigation of using multi-layer PCMs in the tubular heat exchanger with periodic heat transfer boundary condition. *Int. J. Heat Mass Transf.* **2020**, *147*, 118970.
16. Rakotondrandisa, A.; Danaila, I.; Danaila, L. Numerical modelling of a melting-solidification cycle of a phase-change material with complete or partial melting. *Int. J. Heat Fluid Flow* **2019**, *76*, 57–71.
17. NASA. NASA to Begin Testing Next Generation of Spacecraft Heat Exchangers. Available online: https://www.nasa.gov/feature/nasa-to-begin-testing-next-generation-of-spacecraft-heat-exchangers (accessed on 24 August 2021).
18. Kim, T.Y.; Hyun, B.S.; Lee, J.J.; Rhee, J. Numerical study of the spacecraft thermal control hardware combining solid–liquid phase change material and a heat pipe. *Aerosp. Sci. Technol.* **2013**, *27*, 10–16.

19. Zhu, X.; Li, X.; Shen, J.; Wang, B.; Mao, Z.; Xu, H.; Feng, X.; Sui, X.; Stable microencapsulated phase change materials with ultrahigh payload for efficient cooling of mobile electronic devices. *Energy Convers. Manag.* **2020**, *223*, 113478.
20. Rubitherm Technologies GmbH. Available online: https://www.rubitherm.eu/en/ (accessed on 14 July 2021).
21. Vasilios, A.; Alan, D.S. Mathematical modeling of melting and freezing processes. *Hemisph. Publ. Corp.* **1993.**